

Turbulence statistics applied to calculate expected turbulence-induced scintillation effects on electro-optical systems in different climate regions

Karin R. Weiss-Wrana
FGAN-FOM, Gutleuthausstr. 1, D 76275 Ettlingen, Germany
Doc.: FGAN-FOM 2005/09

ABSTRACT

The refractive-index structure parameter C_n^2 is the parameter most commonly used to describe the optically active turbulence. In the past, FGAN-FOM carried out long-term experiments in moderate climate (Central Europe, Germany), arid (summer), and semiarid (winter) climate (Middle East, Israel). Since C_n^2 usually changes as a function of time of day and of season its influence on electro-optical systems should be expressed in a statistical way. We composed a statistical data base of C_n^2 values. The cumulative frequency of occurrence was calculated for a time interval of two hours around noon (time of strongest turbulence), at night, and around sunrise (time of weakest turbulence) for an arbitrarily selected period of one month in summer and in winter. In October 2004 we extended our long-term turbulence experiments to subarctic climate (North Europe, Norway). First results of our turbulence measurement over snow-covered terrain indicate C_n^2 values which are similar or even higher than measured values in Central European winter. The statistical data base was used to calculate the expected turbulence-induced aperture-averaged scintillation index for free-space optical systems (FSO system) in different climates. The calculations were performed for commercially available FSO systems with wavelength of 785 nm and 1.55 μm respectively and with aperture diameters of the receiver of 60 mm and 150 mm for horizontal path at two heights, 2.3 m and 10 m above ground.

Keywords: Atmospheric turbulence, structure parameter of index of refraction C_n^2 , scintillation index, aperture averaging, scintillometer, FSO system

1. INTRODUCTION

Atmospheric turbulence causes intensity fluctuations, scintillation, in the focal plane of a receiver that affects the signal to noise ratio of sensors. The performance of a free-space optical communication system (FSO) can be significantly diminished by the turbulence-induced scintillation resulting from laser beam propagation through the atmosphere. Especially scintillation can lead to power losses at the receiver and possibly to fading of the receiver signal below a prescribed threshold. FGAN-FOM has extended its long-term turbulence measurements to subarctic climate, in northern Norway. In October 2004 we installed a laser scintillometer along an optical path length of 126 m at a height of 3 m over terrain with subarctic vegetation. During winter season 2004/2005, the observation height over snow-covered ground varied between 2.2 m and 2.65 m due to snowfall.

We used our turbulence statistics to calculate the square root of the expected turbulence induced scintillation index or intensity fluctuation. Calculations were performed for two commercially available FSO systems with a wavelength of 785 nm and $\lambda = 1.55 \mu\text{m}$ with aperture diameters of the receiver of 60 mm and 150 mm along a horizontal path at a low height of 2.3 m and at 10 m height, respectively. For a horizontal path the case of a divergent beam was considered indicating the behaviour of a point source or spherical wave. The scintillation index was obtained from equations derived by Andrews et al.¹. We applied the formula with zero inner scale, which neglects both the inner-scale and the outer-scale effects on scintillation. The selected C_n^2 values correspond to a cumulative frequency of 90 % of observed values during daytime in arid summer (overall strongest turbulence), Central Europe winter and subarctic winter (weakest turbulence at noon), and during winter nights in Central Europe (overall weakest turbulence). The calculations were performed for all FSO systems and two altitudes above ground. C_n^2 was scaled with an exponent of $-4/3$ with altitude during daytime (unstable conditions) and $-2/3$ with altitude at night (stable condition), near sunrise (neutral condition), and over snow-layered terrain (stable and neutral conditions). Since the daytime height scaling with $-4/3$ takes a cloud-free sky for granted, a $-2/3$ exponent might be more realistic for Central Europe winter conditions with low temperature difference between ground and overlaying air and frequently cloud covered sky. Hence we investigated the influence of the selected exponent on the expected aperture-averaged intensity fluctuations of FSO systems.

2. THEORY

2.1 Height scaling of C_n^2

With increasing height h C_n^2 decreases up to an altitude of 3 to 5 km. It then increases to a maximum near 10 km, after which it rapidly decreases with increasing altitude. Experiments up to 100 m elevation support among others the model of Tatarski²

$$C_n^2(h) = C_n^2(h_0) \cdot (h/h_0)^{-4/3} \quad \text{daytime:} \quad \text{unstable, free convection} \quad (1)$$

$$C_n^2(h) = C_n^2(h_0) \cdot (h/h_0)^{-2/3} \quad \text{near sunrise and sunset:} \quad \text{neutral conditions} \quad (2)$$

$$\text{night:} \quad \text{stable conditions.}$$

It should be pointed out that stable conditions also apply to specific daytime conditions with warm air over cold ground, e.g. over snow-covered terrain³. Height scaling during daytime with an $-4/3$ exponent is limited to cloud-free sky³. In the case of very low solar irradiance, like cloudy sky during winter in moderate climate, a height scaling with a $-2/3$ exponent might be more realistic during daytime winter⁴.

2.2 Theory of Scintillation

The intensity fluctuation resulting from propagation through turbulence is called scintillation. The variance of the log-amplitude fluctuations, σ_A^2 , can be related to C_n^2 . For a horizontal optical path the case of a divergent beam will be considered that acts like a point source or a spherical wave. Assuming constant C_n^2 , which characterises a horizontal path, σ_A^2 can be calculated for a spherical wave as^{1,5}

$$\sigma_A^2(L) = 0.124 \cdot k^{7/6} L^{11/6} C_n^2 \quad (3)$$

with wavenumber $k = 2\pi/\lambda$ and optical path length L .

The normalized intensity variance σ_I^2 , or scintillation index, is defined by

$$\sigma_I^2 = \frac{\langle [I - \langle I \rangle]^2 \rangle}{\langle I \rangle^2} \quad (4)$$

The relation between the log-amplitude variance and the scintillation index is given by

$$\begin{aligned} \sigma_I^2 &= \exp(\sigma_{\ln I}^2) - 1 = \exp(4\sigma_A^2) - 1 \approx 4\sigma_A^2 & \sigma_A^2 \ll 1 \\ \sigma_I^2 &= 0.5 k^{7/6} L^{11/6} C_n^2 = \beta_0^2 \end{aligned} \quad (5)$$

where β_0^2 is the Rytov variance for a spherical wave. The Rytov variance is linearly proportional to C_n^2 and approximatively proportional to the square of the optical path length L . The wavelength dependence indicates a general feature of turbulence effects: turbulence effects are more severe for shorter wavelengths.

This formula can be applied as long as the variance of log amplitude does not become larger than the limit imposed by the Rytov approximation, $\sigma_A^2 \ll 1$. In agreement with the Rytov approximation, the variance β_0^2 increases linearly with C_n^2 only for low levels of turbulence. For higher levels, the experimental variance approaches a constant and indeed decreases slightly for still higher levels of turbulence. This behaviour is known as the saturation of scintillation.

For strong path-integrated turbulence, approximate expressions for calculation of the variance of normalized intensity fluctuations were derived by Churnside⁵ and Andrews et al¹:

Andrews et al.¹ derived formulas to calculate σ_I^2 which are valid for weak up to strong turbulence conditions. They assumed that the normalized irradiance can be expressed as $I = x \cdot y$, where x and y are statistically independent random quantities:

x arises from large-scale turbulent eddy effects (refractive radius $R_{\text{ref}} > \text{Fresnel zone } (L/k)^{1/2}$) and y from statistically independent small-scale eddy effects (diffractive radius $R_{\text{diff}} < (L/k)^{1/2}$).

The total scintillation index takes the form

$$\sigma_I^2 = \exp(\sigma_{\ln I}^2) - 1 = \exp(\sigma_{\ln x}^2 + \sigma_{\ln y}^2) - 1 \quad (6)$$

where $\sigma_{\ln x}^2$ and $\sigma_{\ln y}^2$ are large-scale and small-scale log-irradiance variances, respectively.

In the case of a spherical wave and neglecting inner scale l_0 (assuming $l_0 = 0$ and outer scale L_0) the scintillation index is then given by

$$\sigma_I^2(L) \cong \exp \left[\frac{0.49 \beta_0^2}{(1 + 1.11 \beta_0^{12/5})^{7/6}} + \frac{0.51 \beta_0^2}{(1 + 0.69 \beta_0^{12/5})^{5/6}} \right] - 1 \quad 0 \leq \beta_0^2 \leq \infty \quad (7)$$

2.3 Aperture averaging

The description of scintillation effects in weak turbulence has been confined to point sources and to point detectors. If the aperture diameter D of a detector is larger than twice the Fresnel zone, $D > 2(L/k)^{1/2}$, the detector will average fluctuations over the aperture, and the signal fluctuation will be less than that of a point receiver. The aperture averaging factor A is given by the ratio of normalized variance of power fluctuations in the receiver plane (irradiance flux variance) over the circular aperture D , $\sigma_I^2(D)$, to that obtained by a ‘‘point’’ aperture (detector with infinitesimally small aperture), σ_I^2 .

The aperture averaged scintillation index σ_I^2 for a spherical wave in the absence of inner scale as derived by Andrews et al.¹ is given by:

$$\sigma_I^2(D) \cong \exp \left[\frac{0.49 \beta_0^2}{(1 + 0.65 \cdot d^2 + 1.11 \beta_0^{12/5})^{7/6}} + \frac{0.51 \beta_0^2 \cdot (1 + 0.69 \cdot \beta_0^{12/5})^{-5/6}}{(1 + 0.9 \cdot d^2 + 0.62 \cdot d^2 \cdot \beta_0^{12/5})^{5/6}} \right] - 1 \quad 0 < \beta_0^2 < \infty \quad (8)$$

with $d = (k \cdot D^2 / 4L)^{1/2}$. In the case that $D = 0$, Eqs (8) reduces to (7).

3. TURBULENCE STATISTICS OVER LAND IN DIFFERENT CLIMATES

Temperature and humidity fluctuations are known to be the primary mechanism affecting the index of refraction and thus the atmospheric turbulence. In daytime, the solar radiation warms up the ground and the air. The temperature gradient between ground and atmosphere results in a turbulent vertical air stream. The temperature gradient is generally greatest at noon when the ground is warmer than the overlying air, thus increasing C_n^2 . Surface roughness increases the temperature gradient and thus C_n^2 . At daytime wind causes air mixing and therefore decreases the inhomogeneity of temperature and humidity and hence decreases C_n^2 . Increasing wind also enhances the dissipation of ground heating, which causes decreasing temperature gradient and C_n^2 . The strength of atmospheric turbulence depends on the net radiation, which is sensitive to cloudiness. When the air temperature is closest to the ground temperature, mainly at sunrise, C_n^2 has a minimum value. At night, there is no heating of the ground hence the temperature gradient is smaller and the vertical heat flux decreases. In the case of laminar temperature flux (horizontal flux), the C_n^2 values are very low. If the temperature of the ground is lower than the air wind causes vertical temperature flux, which results in turbulent flux and strong turbulence of short duration. This results in a strong oscillation of C_n^2 values, an effect that is known as intermittence. Higher wind velocity increases this effect. Intermittence can be observed mainly at night in winter and over snow-covered ground.

3.1 Measurement of C_n^2 values

Measurements of C_n^2 values have been performed with identical laser scintillometers (SLS20, Scintec AG, Germany) in moderate climate, Central Europe, Germany, and in arid/semiarid climate, Middle East, Negev, Israel. The scintillometer provided C_n^2 values integrated over an optical path length of 100 m. In Central Europe C_n^2 values were measured at a height of 1.25 m over grassland (weighted toward the centre of the path) and in Middle-East at a height of 2.3 m above ground without vegetation (only stones and soil). All data were collected continuously for a period of at least one year at a time resolution of 5 minutes. The measurements are described in detail in Weiss-Wrana and Balfour⁶. In October 2004 FGAN-FOM started a long-term turbulence measurement with an identical laser scintillometer in a subarctic climate region, North Europe, Norway. The scintillometer was installed with an optical path length of 126 m at an observation height of 3 m over terrain with low vegetation. During winter season 2004/2005 the height over snow-covered ground varied between 2.2 m and 2.65 m, due to snowfall.

Arid and semiarid climate

Examples of the diurnal cycle of C_n^2 values measured during an arbitrarily chosen summer and winter month in arid (summer) and semiarid (winter) climate, are plotted in Figure 1. During summer there was no overcast sky and the ground was dry. All days show the same characteristic diurnal cycle of C_n^2 . Around noon the atmospheric turbulence was strongest, rising to values of about $8 \cdot 10^{-13} \text{ m}^{-2/3}$. Around sunrise, when the temperature stratification of the atmosphere was stable, the daily variation indicates a distinct minimum of C_n^2 with values of about $1 \cdot 10^{-15} \text{ m}^{-2/3}$. During winter there was precipitation. Due to lower solar irradiance, the maximum of C_n^2 was reduced to values $\leq 5 \cdot 10^{-13} \text{ m}^{-2/3}$. The noon maximum changed by a factor of about 2.5 during the year. At daytime, overcast sky additionally reduced the temperature gradient and hence C_n^2 values. Clouds lead to a 1-2 magnitude reduction in the noon magnitudes. The diurnal cycles indicate a significant variability of the C_n^2 values due to changing cloudiness, but the characteristic diurnal pattern can still be recognized.

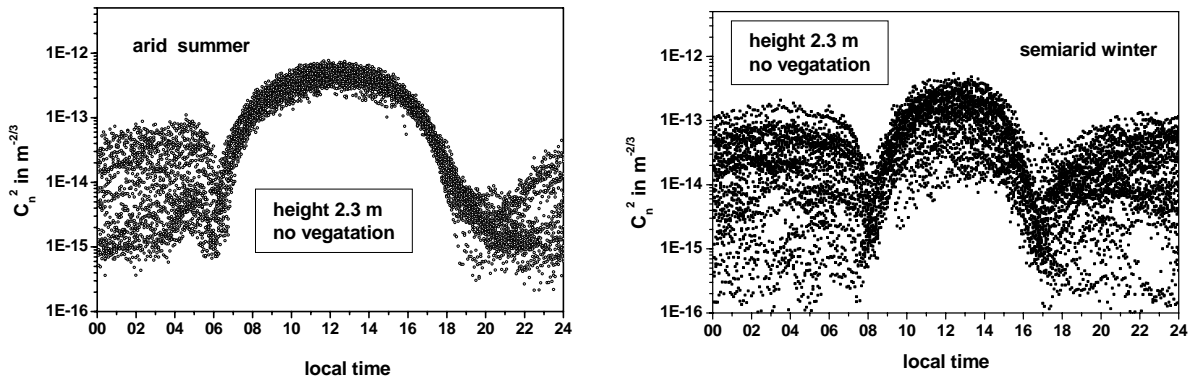


Fig. 1: Diurnal cycle of C_n^2 values measured in arid/semiarid climate, Middle East, at a height of 2.3 m above ground without vegetation during a period of one month during different seasons. Left hand graph: summer August 1999, right hand graph: winter January 2000.

Moderate climate

Examples of the diurnal cycle of C_n^2 values measured during an arbitrarily chosen summer and winter month in moderate climate, Central Europe (Germany), are plotted in Figure 2. In Central Europe, the weather situation can significantly change over a short period, for this reason C_n^2 values show large variance. Nevertheless, the characteristic pattern of the daily variation is perceptible during summer. Winter behaviour is quite different from that of arid climate. Air temperature is significantly lower, causing a very small temperature gradient and hence weak turbulence even during sunny days. Most of the C_n^2 values are $< 1 \cdot 10^{-13} \text{ m}^{-2/3}$. Intermittence is likely which results in oscillating C_n^2 values, hence single large C_n^2 values up to $2 \cdot 10^{-12} \text{ m}^{-2/3}$, corresponding to very strong turbulence, do appear. A characteristic diurnal pattern is no longer identifiable.

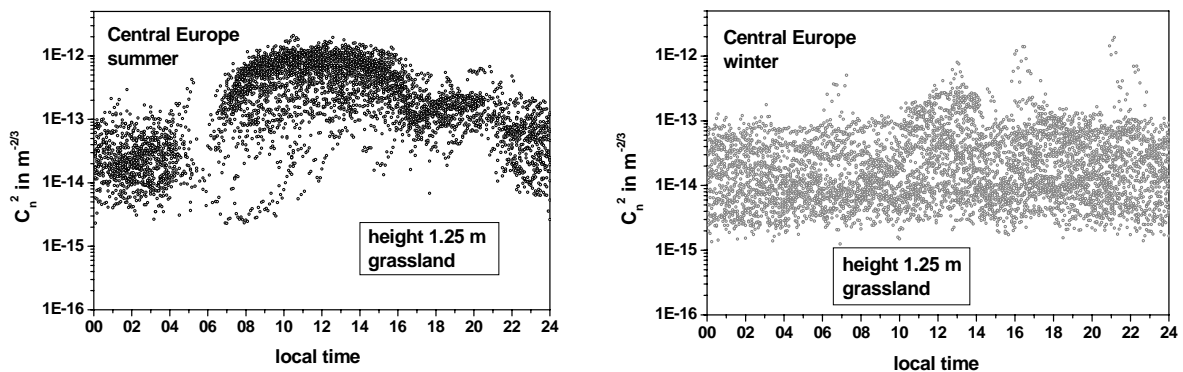


Fig. 2: Diurnal cycle of C_n^2 values measured in moderate climate, Central Europe, at a height of 1.25 m above grassland during a period of one month during different seasons. Left hand graph: summer July 1999, right hand graph: winter January 2000.

Subarctic climate

First results of diurnal cycle measurements of C_n^2 values measured during an arbitrarily chosen winter month, February 2005, above snow-covered terrain in subarctic climate, North Europe (Norway) are plotted in Figure 3. All of February the height of the laser beam above snow-covered ground was about 2.3 m. Measured air temperature at 2.5 m above snow varied between -15°C and $+5^\circ\text{C}$. The measured data featured comparatively high C_n^2 values. Andreas et al.⁷ have measured significantly smaller C_n^2 values over snow-covered drifting sea ice at a height of 3 m, $C_n^2 < 10^{-13} \text{ m}^{-2/3}$. Compared to our turbulence measurement in Central European winter (Figure 2 left hand graph), C_n^2 values over snow-covered ground in North Europe display a larger variability.

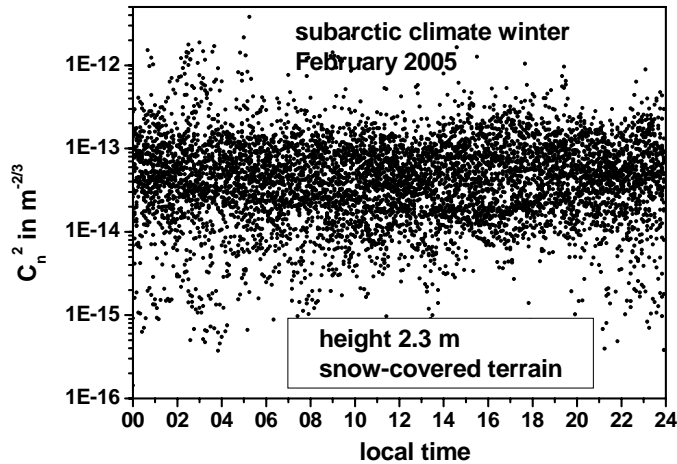


Fig. 3: Diurnal cycle of C_n^2 values measured in subarctic climate, North Europe, at a height of 2.3 m above snow-covered terrain.

3.2 Cumulative frequency of occurrence

Since the atmospheric parameters and hence the atmospheric turbulence usually change as a function of time of day and of season their influence on the effectiveness of electro-optical systems should be expressed in a statistical way. To provide a statistical data base of atmospheric turbulence, the cumulative frequency of occurrence was calculated for a time interval of one month for all climates. Since the diurnal run of C_n^2 values varies by more than one order of magnitude, the calculation of turbulence effects demands a more detailed statement on the expected atmospheric turbulence strength versus the time of day. The cumulative frequency of occurrence was calculated for two-hours time intervals during three selected times of the day: during daytime around noon (11:00 – 13:00 local time), during nighttime around midnight (0:00 – 2:00 local time) and around sunrise. It should be noted that the statistics does not include doubtful single events. As an example for highest and lowest atmospheric turbulence strength, one summer and one winter month in arid and moderate climates were selected and analysed (Weiss-Wrana⁸). The comparison of C_n^2 values measured at different heights makes height scaling necessary. All C_n^2 values were scaled to the height of the measurement in Central Europe, 1.25 m above ground. In Middle East C_n^2 values were scaled at daytime with an $-4/3$ exponent, and at night and near sunrise with an $-2/3$ exponent. In northern Norway, C_n^2 values over snow-covered terrain were scaled with an $-2/3$ exponent, as already mentioned in chapter 2.1.

The cumulative frequency of occurrence for arid, semiarid climate (Middle East), moderate climate (Central Europe) and subarctic climate (North Europe) were plotted in Figures 4, 5 and 6, respectively.

In arid climate, there is a significant difference between winter and summer and between noon, night and sunrise, respectively. In summer, at noon, 90 % of the evaluated data show $C_n^2 > 1 \cdot 10^{-12} \text{ m}^{-2/3}$, very strong turbulence. In winter (semiarid climate) however, 80 % of evaluated data show $1 \cdot 10^{-13} < C_n^2 < 1 \cdot 10^{-12} \text{ m}^{-2/3}$, strong and very strong turbulence.

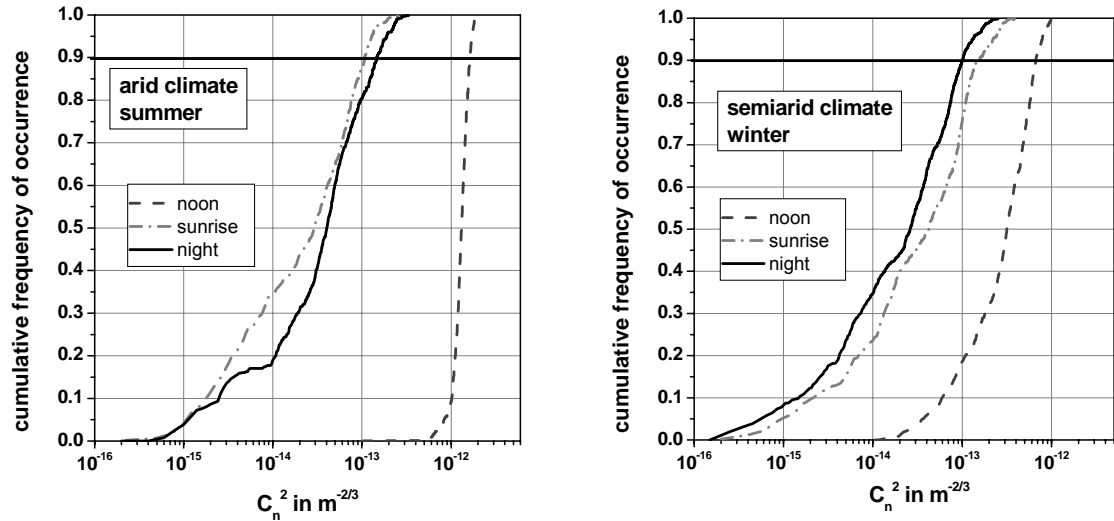


Fig. 4: Cumulative frequency of occurrence of evaluated C_n^2 values measured for a time period of one month during different seasons and different time of day (noon, sunrise and midnight) in arid/semiarid climate (Middle East, Israel). Values are scaled to 1.25 m above ground.

In Central Europe, in summer at noon about 17 % of evaluated data indicate $C_n^2 > 1 \cdot 10^{-12} \text{ m}^{-2/3}$, and 65 % indicate $1 \cdot 10^{-13} < C_n^2 < 1 \cdot 10^{-12} \text{ m}^{-2/3}$, whereas in winter at noon only 23 % of evaluated data show $C_n^2 > 1 \cdot 10^{-13} \text{ m}^{-2/3}$.

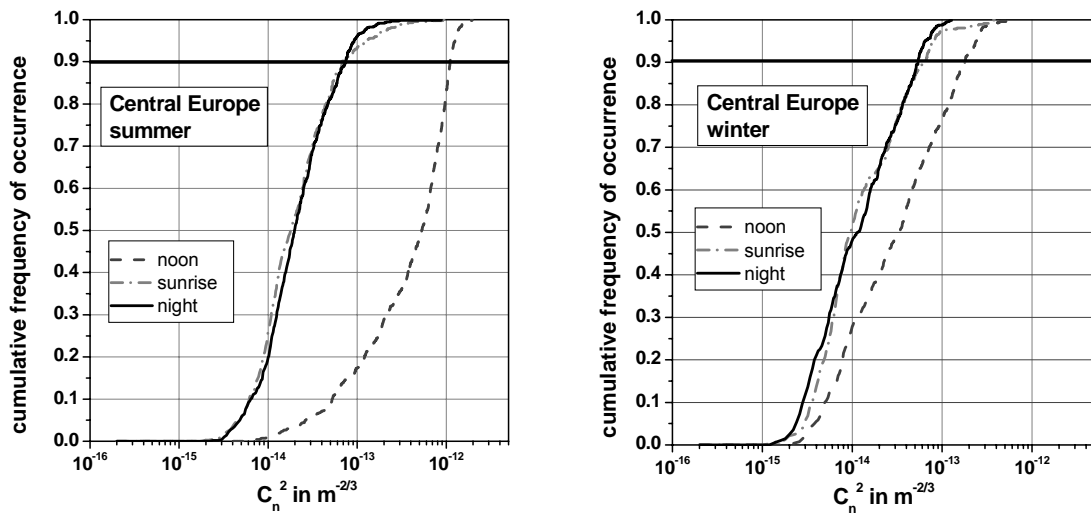


Fig. 5: Cumulative frequency of occurrence of C_n^2 values measured for a time period of one month during different seasons and different time of day (noon, sunrise and midnight) in moderate climate (Central Europe, Germany). Values were measured at 1.25 m above grassland.

In winter in subarctic climate C_n^2 values measured during night can exceed the values measured at noon, see Figure 6. In February 2005, at night 33 % of C_n^2 values are larger than $1 \cdot 10^{-13} \text{ m}^{-2/3}$ whereas at noon hours only 20 % of evaluated data indicate $C_n^2 > 1 \cdot 10^{-13} \text{ m}^{-2/3}$.

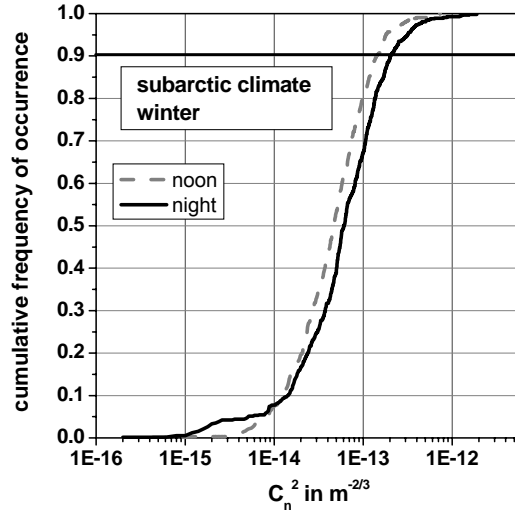


Fig. 6: Cumulative frequency of occurrence of C_n^2 values measured for a time period of one winter month, February 2005, during different time of day (noon and midnight) in subarctic climate (North Europe, Norway) scaled to 1.25 m above snow-covered terrain.

The C_n^2 values corresponding to a cumulative frequency of occurrence of 90 % are listed in Table 1.

climatic conditions		measured C_n^2 -values (in $m^{-2/3}$) corresponding to cumulative frequency of occurrence of 90 %		
climate, geographic location	season	noon 11:00 – 13:00	night 0:00- 02:00	sunrise
arid/semiarid, Middle East soil and stones, height scaled 1.25 m	summer	$1.6 \cdot 10^{-12}$	$1.5 \cdot 10^{-13}$	$1.1 \cdot 10^{-13}$
	winter	$6.7 \cdot 10^{-13}$	$1.0 \cdot 10^{-13}$	$1.5 \cdot 10^{-13}$
moderate, Central Europe grassland, height 1.25 m	summer	$1.1 \cdot 10^{-12}$	$7.4 \cdot 10^{-14}$	$6.7 \cdot 10^{-14}$
	winter	$1.8 \cdot 10^{-13}$	$5.4 \cdot 10^{-14}$	$6.3 \cdot 10^{-14}$
subarctic, North Europe snow-covered terrain, height scaled 1.25 m	winter	$1.4 \cdot 10^{-13}$	$2.0 \cdot 10^{-13}$	

Table 1: C_n^2 values corresponding to a cumulative frequency of occurrence of 90 % measured during different times of day during different seasons in different climates: arid/semiarid climate, moderate climate, and subarctic climate at 1.25 m above ground.

The C_n^2 values corresponding to strongest and weakest daytime turbulence (arid summer respectively Central European winter), weakest turbulence at night (Central Europe winter), as well as over snow-covered terrain (subarctic winter at noon) were selected and scaled to heights of 2.3 m and 10 m above ground. As already mentioned in chapter 2.1 a height scaling with a $-2/3$ exponent might be more realistic during daytime winter in Central Europe.

climate	C_n^2 -values (in $m^{-2/3}$) corresponding to cumulative frequency of occurrence of 90 % scaled to a height of 2.3 m and 10 m above ground		
	height scaling	height 2.3 m	height 10 m
arid climate, summer noon	$h^{-4/3}$	$7.0 \cdot 10^{-13}$	$1.0 \cdot 10^{-13}$
moderate climate, winter noon	$h^{-4/3}$	$7.9 \cdot 10^{-14}$	$1.1 \cdot 10^{-14}$
	$h^{-2/3}$	$1.2 \cdot 10^{-13}$	$4.5 \cdot 10^{-14}$
moderate climate, winter night	$h^{-2/3}$	$3.6 \cdot 10^{-14}$	$1.4 \cdot 10^{-14}$
subarctic climate, winter noon, snow	$h^{-2/3}$	$9.3 \cdot 10^{-14}$	$3.5 \cdot 10^{-14}$

Table 2: Selected C_n^2 values scaled to heights of 2.3 and 10 m.

4. CALCULATION OF EXPECTED APERTURE AVERAGED INTENSITY FLUCTUATION FOR FSO SYSTEMS IN DIFFERENT CLIMATIC REGIONS

The performance of a free-space optical communication system can be significantly diminished by the turbulence-induced scintillation resulting from laser beam propagation through the atmosphere. Specially, scintillation can lead to power losses at the receiver and possible fading of the receiver signal below a prescribed threshold. Prediction of turbulence-induced fading of the laser beam intensity of FSO systems in the plane of the sensor optics is important for system design of FSO systems.

We applied our turbulence statistics to calculate the expected turbulence-induced aperture-averaged scintillation index along a horizontal path at heights of 2.3 m and 10 m above ground for the following FSO systems

wavelength $\lambda = 0.785 \mu\text{m}$	aperture diameter $D = 60 \text{ mm}$
wavelength $\lambda = 0.785 \mu\text{m}$	aperture diameter $D = 150 \text{ mm}$
wavelength $\lambda = 1.55 \mu\text{m}$	aperture diameter $D = 60 \text{ mm}$
wavelength $\lambda = 1.55 \mu\text{m}$	aperture diameter $D = 150 \text{ mm}$

A quantity for indicating fading is the square root of the scintillation index, $\sigma_I(D)$ or intensity fluctuation. The corresponding $\sigma_I(D)$, as a function of path length L are plotted in Figure 7 for FSO systems with $\lambda = 785 \text{ nm}$, and in Figure 8 for systems with $\lambda = 1.55 \mu\text{m}$, respectively. The graphs on the left hand correspond to calculations with $D = 60 \text{ mm}$ and the graphs on the right hand to calculations with $D = 150 \text{ mm}$. The top graphs correspond to the calculations with C_n^2 values scaled to a height of 2.3 m above ground and the bottom graphs to C_n^2 values scaled to 10 m above ground.

$\sigma_I(D)$ increases up to a peak value, and decreases slightly with further increasing path length. Since the aperture-averaged intensity fluctuation $\sigma_I(D)$ is non-linearly affected by both the spherical Rytov variance β_0^2 , proportional to L and C_n^2 , and the factor d , proportional to aperture diameter D and inversely proportional to the square of L , $\sigma_I(D)$ as a function of L shows different behaviour for different C_n^2 values and different aperture diameters D .

Comparing the left hand and the right hand graphs it can be seen, that a larger aperture diameter decreases the expected intensity fluctuations, and the expected peak fluctuation will occur at larger path lengths. Comparing $\sigma_I(D)$ values expected for strongest turbulence conditions with weakest turbulence conditions, one has to expect a significantly steeper increase of $\sigma_I(D)$ in strong conditions with peak fluctuation occurring at shorter path lengths with a lower peak value.

As long as the Rytov criterion is satisfied an increase in path length or in C_n^2 values does always yield a larger $\sigma_I(D)$ value. In each graph there are crossovers of the various expected intensity fluctuations. This occurs at path lengths L_{cross} where the Rytov criterion is still satisfied for weaker turbulence while for stronger turbulence $\sigma_I(D)$ has already exceeded its maximum and is decreasing with increasing L . It should be noted out that for path lengths $L > L_{\text{cross}}$ the expected intensity fluctuations under weaker turbulence conditions are larger than under stronger turbulence. The crossover path length L_{cross} depends on C_n^2 and the aperture diameter D . Smaller C_n^2 values and larger aperture diameters D cause a shift of L_{cross} towards larger values. This effect can be seen when comparing the left hand and the right hand graphs and the corresponding top and bottom graphs of Figure 7 and Figure 8, respectively.

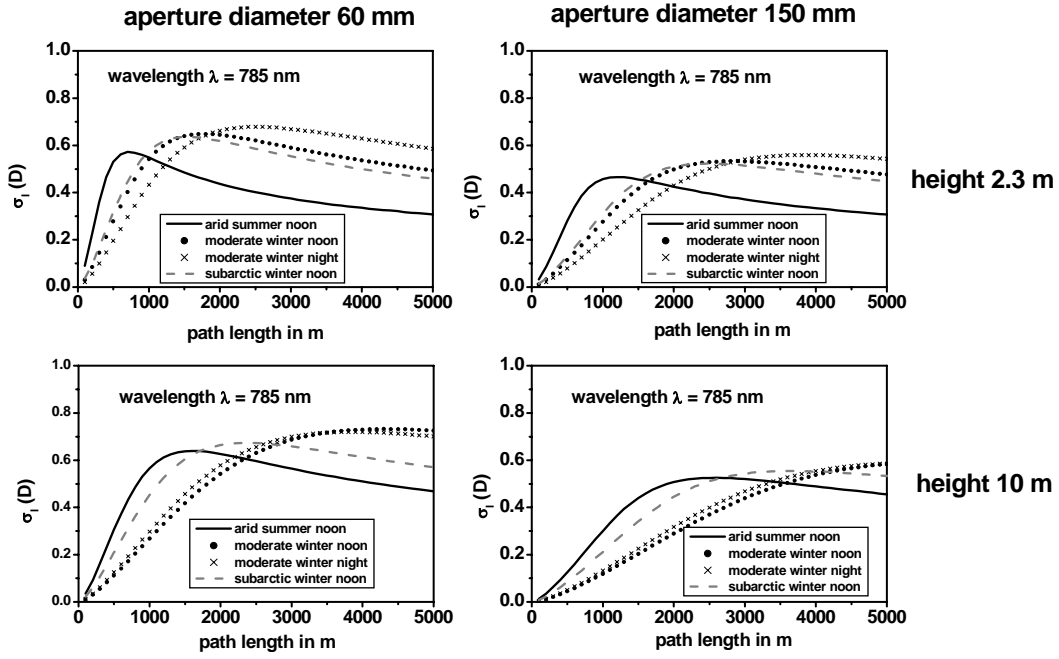


Fig. 7: The square root of aperture-averaged scintillation index, $\sigma_I(D)$, in the plane of the aperture of FSO systems with wavelength $\lambda = 0.785 \mu\text{m}$ and aperture diameter 60 mm (left hand graphs) and 150 mm (right hand graphs) at 2.3 m (top graphs) and 10 m above ground (bottom graphs) calculated for four selected C_n^2 values.

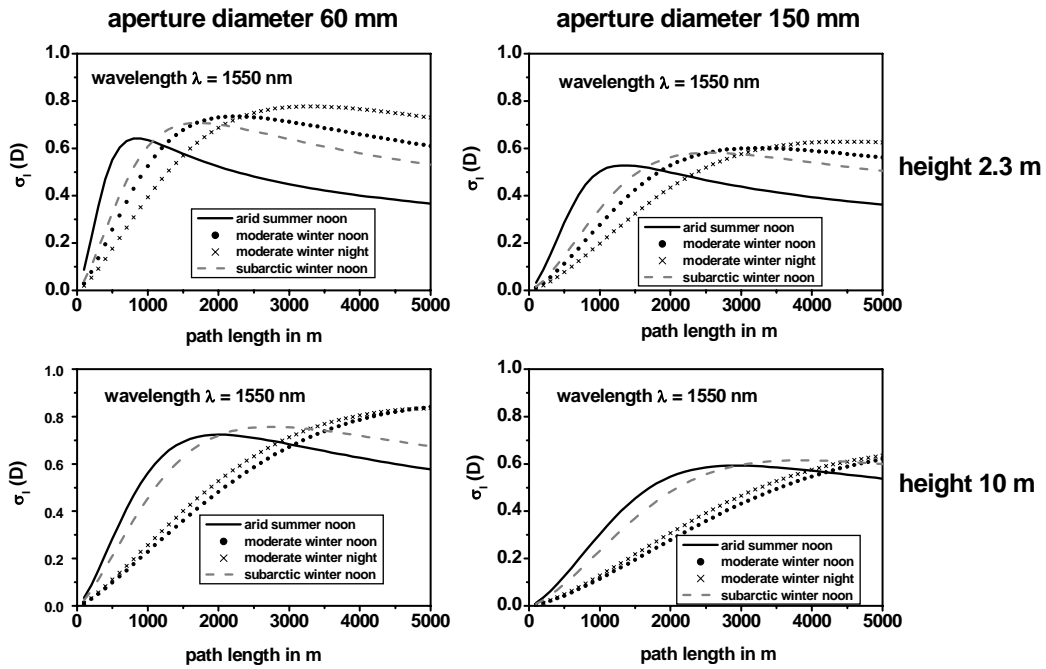


Fig. 8: Same as Figure 7, for wavelength $\lambda = 1.55 \mu\text{m}$.

Figure 9 compares the $\sigma_I(D)$ values, calculated for the short-wave and the long-wave FSO system with aperture diameter of 60 mm (solid line) and of 150 mm (dashed line) as expected under strongest turbulence conditions, at a height of 2.3 m (left hand graph) and 10 m (right hand graph) above ground. As long as the Rytov criterion is satisfied for both systems, the expected intensity fluctuation for the 785 nm FSO system is slightly larger than that for the 1.55 μm FSO system. For longer path lengths however, $L > L_{\text{cross}}$ the expected intensity fluctuations for the 785 nm FSO system are smaller than that for the 1.55 μm FSO system. The use of a larger aperture diameter (dashed curves) results in significantly smaller intensity fluctuations. The aperture-averaging effect depends on the selected wavelength and the selected C_n^2 values. It can be seen that for the short-wave FSO system under strong turbulence conditions at low altitude (black lines in left hand graph) the aperture-averaging effect becomes negligible small for path lengths $L > 2000$ m. For the long-wave FSO system under weaker turbulence conditions (grey lines in right hand graphs) however there is still a aperture-averaging effect for path lengths up to 5000 m.

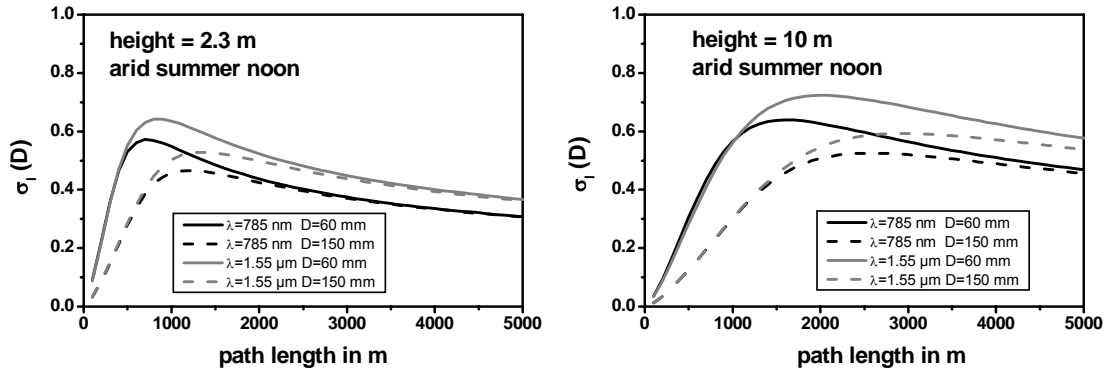


Fig. 9: Comparison of the expected square root of turbulence-induced scintillation index $\sigma_I(D)$ calculated for two FSO systems, $\lambda = 785$ nm and $\lambda = 1.55$ μm with aperture diameter 60 mm and 150 mm for a horizontal path at a height of 2.3 m (left hand graph) and 10 m (right hand graph) for turbulence conditions arid summer at noon.

Since C_n^2 scales with an exponent of $-4/3$ with altitude only for cloud-free skies, C_n^2 values, measured in moderate winter at noon (low solar irradiance and prevalent cloudy sky), were also scaled with an exponent of $-2/3$. Figure 10 shows the influence of the scaling exponent on $\sigma_I(D)$. At lower altitude, there is only little difference, while at an altitude of 10 m the selected exponent of $-4/3$ or $-2/3$ results in a significant difference. The steep decrease of C_n^2 with exponent $-4/3$ might lead to too optimistic prediction of $\sigma_I(D)$. A more realistic model of C_n^2 altitude dependence during daytime with cloud covered sky should be something in between $-4/3$ and $-2/3$.

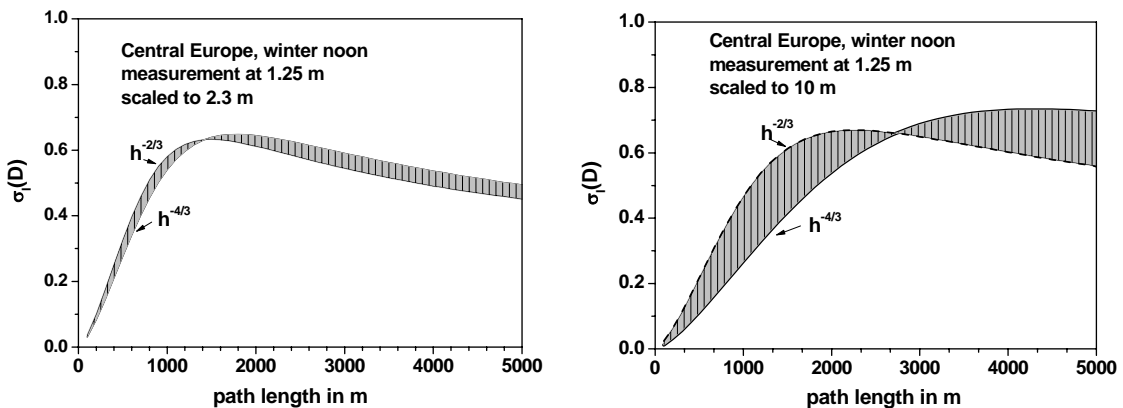


Fig. 10: The impact of height scaling exponent of $-4/3$ and $-2/3$, on the square root of turbulence-induced scintillation index $\sigma_I(D)$, calculated for a height of 2.3 m (left hand graph) and 10 m (right hand graph).

5. CONCLUSIONS

In the past FGAN-FOM composed a statistical data base of C_n^2 values which were measured during long-term experiments in moderate climate in Central Europe, Germany, and in arid (summer) and semiarid (winter) climate in Middle East, Israel. It provides differentiated statements of the cumulative frequency of occurrence for different times of the day during different seasons in both climates. The cumulative frequency of occurrence was determined for a time interval of two hours around noon (strongest turbulence), and at night and around sunrise (weakest turbulence) for an arbitrarily selected period of one month in summer and in winter. FGAN-FOM extended its long-term turbulence experiments to a subarctic climate (North Europe, Norway). Since November 2004, we have measured the path integrated C_n^2 values with an identical laser scintillometer along an optical path length of 126 m over snow-covered terrain. The measurements indicate a large variability of C_n^2 values which are significant larger than those measured by Andreas et al.⁷ over snow-covered drifting ice.

The performance of a free-space optical communication system (FSO system) can be significantly degraded by the turbulence-induced scintillation resulting from laser beam propagation through the atmosphere. Especially, scintillation can lead to power losses at the receiver and possible fading of the receiver signal below a prescribed threshold. Prediction of turbulence-induced fading of the laser beam intensity in the plane of the sensor optic of FSO systems is important for the design of systems. A quantity for indicating fading is the square root of the scintillation index, $\sigma_I(D)$ or intensity fluctuation. We applied our turbulence statistics to calculate the square root of expected aperture-averaged scintillation index, $\sigma_I(D)$ for FSO systems with a wavelength $\lambda = 0.785 \mu\text{m}$ and $\lambda = 1.55 \mu\text{m}$ and aperture diameter $D = 60 \text{ mm}$ and 150 mm .

For the calculations of $\sigma_I(D)$ we disposed the method of Andrews et al. We applied the formula with zero inner scale, which neglects both the inner-scale and the outer-scale effects on scintillation. The calculations were carried out for C_n^2 values corresponding to a cumulative frequency of 90 % indicating strongest and weakest daytime turbulence (arid summer and Central European winter, respectively), weakest turbulence at night (Central Europe winter), as well as over snow-covered terrain (subarctic winter at noon). C_n^2 was scaled to a height of 2.3 m and 10 m above ground at daytime with an $-4/3$ exponent (unstable conditions), at night and near sunrise and over snow-layered terrain with an $-2/3$ exponent (neutral or stable conditions). For Central Europe winter at noon we additionally scaled the C_n^2 values with an exponent of $-2/3$.

$\sigma_I(D)$ as a function of path length L increases up to a peak value, and decreases slightly with further increasing L . The peak value and the path length where it occurs depend on the wavelength, C_n^2 , and aperture diameter. As long as the Rytov criterion is satisfied one expects larger intensity fluctuation for short-wave systems than for long-wave FSO systems. But if the Rytov criterion is satisfied only for weaker turbulence condition, or for longer wavelength, while for stronger turbulence, or shorter wavelength, $\sigma_I(D)$ has already exceeded its maximum and is decreasing with increasing L , there will be a cross-over of the devolution of the corresponding $\sigma_I(D)$ values at a path length called L_{cross} . For path lengths $L > L_{\text{cross}}$ the expected intensity fluctuation under weaker turbulence conditions is larger than under stronger turbulence. L_{cross} depends on C_n^2 , the aperture diameter and on the wavelength. Smaller C_n^2 values and larger aperture diameter D causes a shift of L_{cross} towards larger values. A larger aperture diameter will decrease the expected intensity fluctuations. The effect of aperture-averaging depends not only on the aperture diameter but also on the wavelength, C_n^2 , and the optical path length, it is decreasing with increasing path length. It should be noted, that the presented results are sensitive to the selected exponent for scaling of C_n^2 with altitude.

A general statement on the applicability of FSO systems with different wavelengths concerning the expected turbulence-induced aperture-averaged intensity fluctuation for different turbulence conditions is scarcely possible. In fact, detailed calculations of expected intensity fluctuations are necessary to make a decision which system (wavelength and aperture diameter) would be most suitable for a specific task.

6. ACKNOWLEDGEMENT

The author wishes to express appreciation to the Norwegian Air Base, Bardufoss, and the FFI, Kjeller, for providing us with an appropriate test site. Special thanks go to the colleagues Frode-Berg Olsen and Tor Høimyr at FFI, Kjeller, and Steinar Bjørkeng at the Norwegian Air Base, Bardufoss, for their invaluable help. Without their assistance, the project in Norway would not have come true.

7. REFERENCES

1. Andrews L.C., Phillips R.L., Hopen C.Y.: *Laser Beam Scintillation with Applications*, SPIE PRESS, Bellingham, Washington, 2001.
2. Tatarski V.I.: *Wave Propagation in a Turbulent Medium*, McGraw-Hill, New York, 1971.
3. Beland R.R.: "Propagation through Atmospheric Optical Turbulence", *The Infrared & Electro-Optical Systems Handbook, Volume 2: Atmospheric Propagation of Radiation*, Smith Editor, SPIE Optical Engineering Press, Bellingham, Washington, 1993.
4. Thiermann V.: private communication (Scintec AG, Germany).
5. Churnside J.H.: "Aperture Averaging of Optical Scintillation in the Turbulent Atmosphere", *Appl. Opt.*, **Vol. 30**, pp. 1982-1993, 1991.
6. Weiss-Wrana K.R., Balfour L.: "Statistical Analysis of Measurements of Atmospheric Turbulence in Different Climates", *Proceedings of SPIE*, **Vol. 4538**, pp. 93-101, 2002, Bericht FGAN-FOM 2001/20.
7. Andreas E.L., Fairall Ch.W., Persson P.O.G., Guest P.S.: "Probability Distributions for the Inner Scale and the Refractive Index Structure Parameter and their Implication for Flux Averaging", *J. Appl. Met.*, **Vol. 42**, pp. 1316-1329, 2003.
8. Weiss-Wrana K.R.: "Influence of Atmospheric Turbulence on Imaging Quality of Electro-Optical Sensors in Different Climates", *Proceedings of SPIE*, **Vol. 5237**, pp. 1-12, 2004, Bericht FGAN-FOM 2003/11.